Journal of Applied Polymer Science

Thermal and mechanical behavior of poly(vinyl butyral)-modified novolac epoxy/multiwalled carbon nanotube nanocomposites

Kavita, Bablu Mordina, R. K. Tiwari
Defence Materials and Stores Research and Development Establishment, Kanpur 208013, India
Correspondence to: B. Mordina (E-mail: mordina_pol@yahoo.ie)

ABSTRACT: The effects of poly(vinyl butyral) (PVB) and acid-functionalized multiwalled carbon nanotube modification on the thermal and mechanical properties of novolac epoxy nanocomposites were investigated. The nanocomposite containing 1.5 wt % PVB and 0.1 wt % functionalized carbon nanotubes showed an increment of about 15°C in the peak degradation temperature compared to the neat novolac epoxy. The glass-transition temperature of the novolac epoxy decreased with increasing PVB content but increased with an increase in the functionalized carbon nanotube concentration. The nanocomposites showed a lower tensile strength compared to the neat novolac epoxy; however, the elongation at break improved gradually with increasing PVB content. Maximum elongation and impact strength values of 7.4% and 17.0 kJ/m^2 were achieved in the nanocomposite containing 1.5 wt % PVB and 0.25 wt % functionalized carbon nanotubes. The fractured surface morphology was examined with field emission scanning electron microscopy, and correlated with the mechanical properties. The functionalized carbon nanotubes showed preferential accumulation in the PVB phase beyond 0.25 wt % loading. © 2015 Wiley Periodicals, Inc. J. Appl. Polym. Sci. **2016**, *133*, 43333.

KEYWORDS: composites; mechanical properties; properties and characterization; thermal properties

Received 12 August 2015; accepted 12 December 2015
DOI: 10.1002/app.43333

INTRODUCTION

The most commonly used epoxy resins are bisphenol A based resins, which are formed via the condensation reaction of bisphenol A with excess epichlorohydrin. Bisphenol A based epoxy resin is the simplest basic form of novolac-based epoxy resin with a low epoxide equivalent. A weak mechanical strength and weak thermal properties are the major limitations of this resin. Multifunctional novolac epoxy resins are superior in numerous ways when compared to bisphenol A and bisphenol F based resin systems, as they generally have higher epoxide equivalent weights; this causes them to show better elevated temperature resistance and strength. Novolac-based epoxy resin is one such multifunctional epoxy resins with a higher epoxide equivalent weight than either bisphenol A or bisphenol F based epoxy resins; this results in a more highly crosslinked structure.[1] The highly crosslinked structure of the final cured resin ultimately results in a high mechanical strength in the final composites. Because of these significant properties, they are used in space shuttle materials, adhesives, coatings, and aerospace applications.[2,3] However, these resins are brittle, and their structural applications are limited because of their high crosslinking density. To diminish the brittleness, the resins are suitably modified to impart flexibility to the resin. The elastomers widely used in the literature for the modification of thermosets are carboxyl-terminated butadiene acrylonitrile (CTBN),[4] vinyl-terminated butadiene acrylonitrile, polyurethane,[5] and so on. Elastomer particles, at some significant concentration while dispersed in a thermoset, change the fracture mechanism and prevent the brittle fracture of the composite by transferring stress from the thermoset to the elastomeric phase and reduce the stress around the crack tip below the crucial point. A thermoplastic polymer, poly(vinyl butyral) (PVB), was also used to modify the viscoelastic and adhesion properties of phenolic and epoxy-based adhesives.[6,7] The mechanical loss of the phenolic–PVB coating (adhesive) was observed to increase up to a 50 wt % PVB content.[6] The adhesive shear, peel strength, cohesive strength, and film-forming ability were also improved with PVB modification.[7] The effects of the elastomeric modifiers on the fracture and toughening behavior of thermosetting resins have been studied by many researchers.[8–14] Sulton and Carry[8] and Bascom *et al.*[10] studied the effect of CTBN on the fracture behavior of bisphenol A based epoxy resin. The fracture toughness and impact strength showed 603.6 and 187.1% improvements in 10 wt % CTBN modified epoxy compared to the neat epoxy.[9] A microscopic study revealed that for optimal properties of the composites, the particle

Additional Supporting Information may be found in the online version of this article

size of the elastomeric modifier should be within a particular size range. Interestingly, elastomeric particles in the size range of a few hundred angstroms led to the enhanced shear deformation of the composite without the formation of a cavity. However, larger particles led to failure of the material at a relatively lower strain value because of the formation of large cracks by the coalescence of cavities.[8] PVB resins have three different functional groups (hydroxyl, acetate, and acetal groups) in their structure, and this often results in superior properties when PVB is used in combination with a thermosetting resin. PVB and novolac epoxy resin in combination find significant importance in ballistic applications because of their incompatible characteristics. The incompatibility of the polymer matrix plays a crucial role in determining the ultimate ballistic performance of the composite because the energy of impact can be easily dissipated by the delamination of the composite layers. At some optimum concentration, PVB improves the toughness of the composites but simultaneously decreases the thermal stability because of the low crosslinking density. The incorporation of a nanofiller, such as carbon nanotubes (CNTs), is the most convenient method for improving the mechanical and thermal properties of the thermosets, as they can lead to a significant change in these properties at very low filler loadings.[15–19] The incorporation of 1 wt % pristine multiwalled carbon nanotubes (MWCNTs) and acid-functionalized multiwalled carbon nanotubes (f-MWCNTs) was observed to cause 58 and 100% improvements in the flexural strength of the epoxy nanocomposites along with improved thermal stability.[16] An enhancement of approximately 10°C in the onset degradation temperature was observed in epoxy nanocomposites at the same MWCNT loading.[18] Moreover, the formation of covalent bonds between the CNTs and polymer matrix resulted in a strong polymer–matrix interaction. Hence, the former was reported to be 10,000 times more resistive than the noncovalent-type nanocomposite.[15] CNTs as the reinforcing filler led to a significant enhancement in the performance of the resulting composites by improving their mechanical properties. It is well known that the ultimate properties of the nanocomposites mostly depend on the dispersion of the nanofiller and their interfacial bonding with the polymer matrix.[20–24] The functionalization of CNTs is the most commonly practiced method for improving the interfacial strength of CNTs with the matrix material. In this study, novolac-based epoxy nanocomposites were investigated for their thermal and mechanical properties. To counter the reduction in the thermal stability of the composites due to PVB addition, f-MWCNTs were used as a nanofiller. To the best of our knowledge, this is the first experimental study on the effects of PVB and CNTs on the thermal and mechanical characteristics of novolac-based epoxy resin.

EXPERIMENTAL

Materials

Phenol was purchased from E. Merck (India), Ltd. (Mumbai). Sodium hydroxide pellets, a 37% aqueous formaldehyde solution, methyl ethyl ketone, pyridine, and acetic anhydride were kindly supplied by Samir Tech.–Chem. Pvt., Ltd. Epichlorohydrin (purity = 99%) and MWCNTs (length = 5–9 μm and diameter = 110–170 nm) were purchased from Sigma Aldrich. The curing agent HY 951 (triethylene tetra amine) was purchased from Huntsman Advanced Materials Pvt., Ltd. (Mumbai, India). PVB was procured from Synpol Pvt., Ltd. (Ahmedabad, India).

Table I. Compositions of the Nanocomposites

Sample designation	Novolac epoxy (wt %)	PVB (wt %)	MWCNTs (wt %)
Neat novolac epoxy	100	—	—
Composite a	99	0.5	0.5
Composite b	98.40	1.5	0.1
Composite c	98.25	1.5	0.25
Composite d	98	1.5	0.5
Composite e	97	2.5	0.5

Synthesis of the Novolac Resin

Novolac resin was synthesized by the reaction of phenol and formaldehyde in an acidic medium (pH 3–3.5). Phenol and formaldehyde were taken in a molar ratio of 1:0.8. The reaction mixture was refluxed and stirred at 90°C for 2–3 h. After completion of the reaction, the viscous resin was separated by the removal of aqueous layer by vacuum distillation. Finally, the resin was dried in a vacuum oven at 70°C for 3–4 h.

Synthesis of the Novolac-Based Epoxy Resin

The phenolic groups of the novolac resins could be readily converted into epoxy groups through reaction with excess epichlorohydrin in the presence of aqueous NaOH.[25] In a typical method, novolac and epichlorohydrin were taken in a 1:6 molar ratio. The reaction mixture was refluxed at 90°C for 6 h with the simultaneous addition of 30% aqueous NaOH solution. After completion of the reaction, the resin was washed several times with hot distilled water to remove excess epichlorohydrin. Finally, the resin was dried at 70°C for 3–4 h in a vacuum oven.

Functionalization of the MWCNTs

The MWCNTs were first sonicated in a 1:3 v/v mixture of concentrated H_2SO_4 and HNO_3 for 2 h to disperse the nanotubes and to wet the nanotube surface by the acid solution. This nanotube dispersion was then refluxed at 100°C for 6 h under magnetic stirring. The f-MWCNTs were separated by filtration and were washed several times with distilled water until a neutral pH was reached. Finally, the f-MWCNTs were dried in a vacuum oven at 50°C for 5–6 h.

Fabrication of the Nanocomposites

Initially, the f-MWCNTs were sonicated in a methyl ethyl ketone solvent. A PVB solution was also prepared with the same solvent. Finally, both solutions were added to the epoxy resin and mixed homogeneously with the help of a high-speed disperser (model T25 D S22, IKA) at 15,600 rpm for 30 min. Afterward, 10% curing agent was mixed homogeneously by mechanical stirring and cast into a mold. The cast composite was cured at room temperature for 24 h followed by postcuring at 100°C for 2 h in an air oven. The neat novolac epoxy based reference sample was also fabricated under similar experimental conditions. The composition of the nanocomposites is shown in Table I.

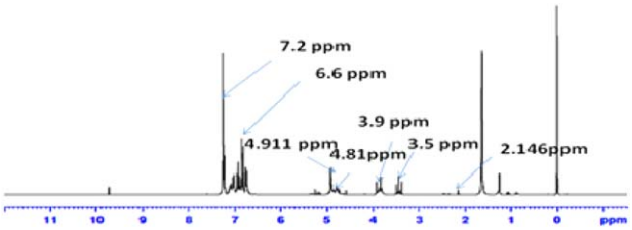

Figure 1. [1]H-NMR spectrum of the novolac resin. [Color figure can be viewed in the online issue, which is available at wileyonlinelibrary.com.]

Characterization

Novolac and novolac epoxy resins were analyzed by [1]H-NMR and Fourier transform infrared (FTIR) spectroscopy to determine the chemical structure. Hydroxyl and epoxide group equivalents were also determined to optimize the epichlorohydrin and curing agent ratio. The neat and functionalized MWCNTs were characterized by FTIR and Raman spectroscopy. The nanocomposites were characterized by thermogravimetric analysis (TGA) and modulated differential scanning calorimetry (MDSC) for the thermal properties. Mechanical properties, namely, the tensile and flexural properties, were investigated with test methods from ASTM D 3039 and ASTM D 790. The Izod impact strength was determined according to ASTM D 256. For each nanocomposite, at least five specimens were tested, and the average of these values was reported as the experimental result. The morphological analysis of the neat MWCNTs and f-MWCNTs and the fracture surfaces of the nanocomposites was performed with field emission scanning electron microscopy (FESEM). Details of the characterization techniques are provided in the Supporting Information.

RESULTS AND DISCUSSION

[1]H-NMR

Figure 1 shows the [1]H-NMR spectra of the synthesized novolac resin. Multiplets observed at δ values of 3.5 and 3.9 ppm were due to the presence of aliphatic protons in the novolac resin. These aliphatic protons corresponded to the ortho–ortho, and para–para methylene units of the novolac resin.[26] Multiplets at a δ value of 4.81 ppm were due to the methylene protons of the —CH_2OH (methylol) groups of the novolac resin, which were formed in small amounts during the synthesis. Singlets arising at δ values of 2.146 and 4.911 ppm were due to methylol —OH and phenolic —OH. NMR peaks at δ values of 6.6 and 7.2 ppm were attributed to the benzene ring protons of the novolac resin.

Figure 2 represents the [1]H-NMR spectra of the novolac epoxy resin. Multiplets at δ values of 2.6 and 2.9 ppm were observed

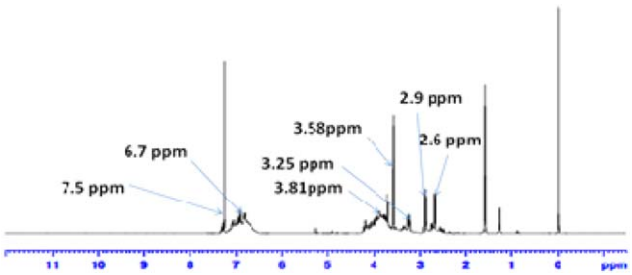

Figure 2. [1]H-NMR spectrum of the novolac epoxy resin. [Color figure can be viewed in the online issue, which is available at wileyonlinelibrary.com.]

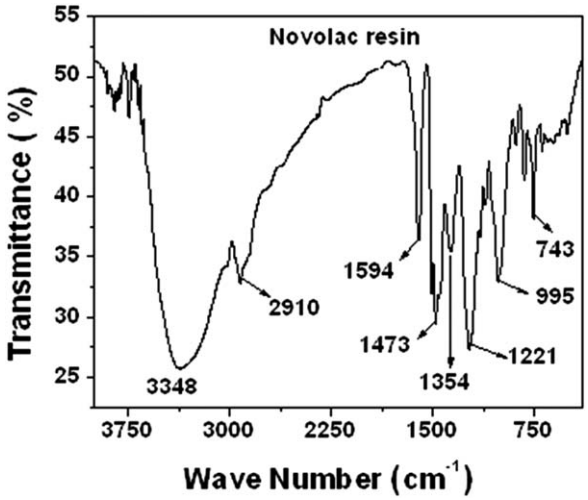

Figure 3. FTIR spectrum of the novolac resin.

due to the presence of aliphatic protons of >CH_2 group attached to the epoxy ring. The multiplet at 3.25 ppm corresponded to the aliphatic proton attached to the >CH group of the epoxy ring. A multiplet of two methylene protons connecting two benzene rings at the para position was observed at a δ value of 3.81 ppm. NMR peaks in the regions of 6.7 and 7.5 ppm appeared due to the aromatic protons of the benzene ring.

FTIR Spectroscopy

The FTIR spectrum of the synthesized novolac resin is shown in Figure 3. The broad absorption peak at 3348 cm^{-1} was due to the presence of stretching vibrations of the phenolic —OH group. The absorption peaks at 1473 and 822 cm^{-1} were attributed to the C=C stretching and —CH bending vibrations of the ortho- and para-substituted phenolic ring.[26] The band at 1221 cm^{-1} was due to the presence of C—O stretching vibrations in the phenolic ring.

Figure 4 shows the FTIR spectrum of the novolac epoxy resin. It was evident from the figure that the broad absorption peak of the novolac resin at 3348 cm^{-1} was reduced in the novolac

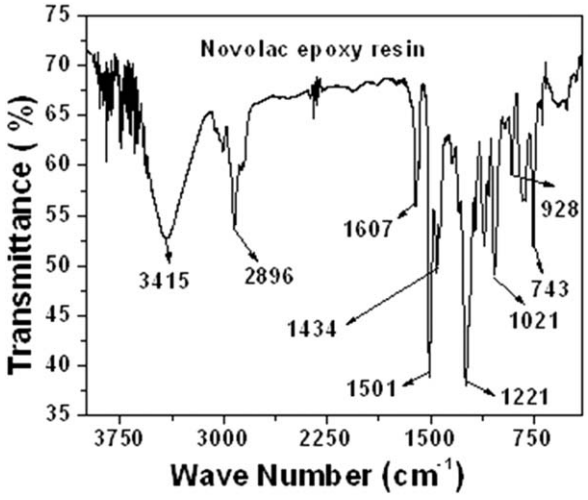

Figure 4. FTIR spectrum of the novolac epoxy resin.

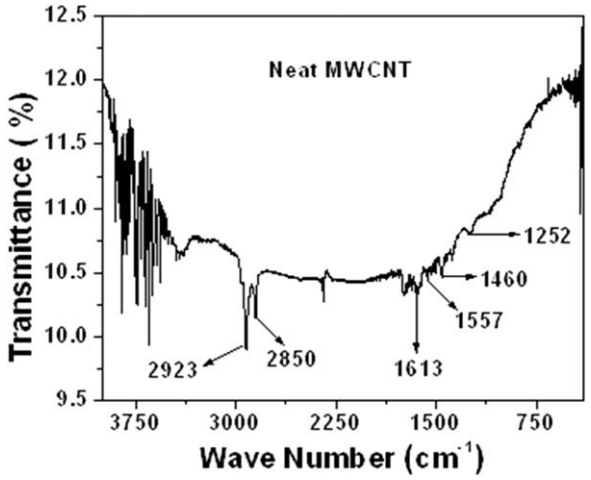

Figure 5. FTIR spectrum of the neat MWCNTs.

epoxy resin. Hence, the reduction in the intensity of the broad —OH peak at 3415 cm^{-1} indicated the conversion of the maximum phenolic —OH group into the epoxide linkage. The absorption bands at 2896 and 1434 cm^{-1} corresponded to the —CH and CH_2 stretching vibrations of the alkane group of the epoxy ring. The aromatic C=C stretching and C—O stretching vibrations of the phenolic ring were observed at 1501 and 1221 cm^{-1}, respectively. The peak at 928 cm^{-1} was due to the presence of the epoxy ring in the synthesized resin and confirmed the formation of epoxy linkages in the novolac epoxy resin.

FTIR spectra of the neat MWCNTs and f-MWCNTs are shown in Figures 5 and 6(a), respectively. In the neat MWCNTs, the absorption band at 2923 and 2850 cm^{-1} corresponded to C—H stretching vibrations. This —CH group originated from imperfections or defects in the MWCNTs developed during the manufacturing process.[27] The absorption peaks at 1460, 1557, and 1613 cm^{-1} corresponded to the C=C stretching vibrations of the aromatic ring.

In the f-MWCNTs, characteristic —OH stretching and the —OH bending of the carboxylic group appeared at 3441 and 995 cm^{-1}. The absorption peak at 1620 cm^{-1} corresponded to the C—C stretching vibrations of the aromatic ring. The absorption bands at 2910 and 1367 cm^{-1} were due to C—H stretching and —C—H rocking vibrations of alkane. The absorption peaks at 1639 and 1100 cm^{-1} were attributed to the C=O and C—O stretching vibrations of the —COOH group; this confirmed the successful acid functionalization of the MWCNTs.

Figure 6(b) represents the FTIR spectra of the reaction product of PVB and f-MWCNTs. The spectra showed C=O and C—O stretching frequencies at 1740 and 1261 cm^{-1}, respectively, for the formation of ester linkages between the f-MWCNTs and PVB resin. The formation of ester linkages was further confirmed by the reduction in the —OH stretching peak intensity of PVB and —COOH group of the f-MWCNTs. The absorption peaks at 2843 and 2923 cm^{-1} corresponded to the —C—H stretching frequency of the $—CH_3$ group of the grafted PVB chains. The absorption bands at 1021 and 1465 cm^{-1} were attributed to the $C—CH_3$ stretching and $—CH_3$ asymmetric bending mode of PVB. A similar type of grafting of poly(lactic acid) to f-MWCNTs was reported in literature.[27] In our study, the resulting esterified product was observed to be insoluble in methyl ethyl ketone (which was used as the solvent in the preparation of the nanocomposites); this led to the poor dispersion of PVB and MWCNTs within the novolac epoxy resin.

Raman Spectroscopy

Figure 7 shows the Raman spectra of the neat MWCNTs and f-MWCNTs. The MWCNTs are basically rolled graphene sheets. Both MWCNTs showed the characteristic Raman peak at 1339 cm^{-1} due to the D band (defect activated peak) of graphene. However, G (first order graphitic peak) and 2D peaks (second order defect activated peak) appeared at 1564 and 2684 cm^{-1} and 1566 and 2687 cm^{-1}, respectively, for the MWCNTs and f-MWCNTs.[28] The D band originated from the sp^3-hybridized vibrational modes of graphene and indicated the presence of defects in the regular graphene structure, whereas the 2D band represented the interlayer interactions between the rolled graphene sheets. The G band arose because of the sp^2 hybridization of the planar graphene sheets. All of the bands appeared at almost identical frequency shifts for both the MWCNTs and f-MWCNTs, but their intensities were different. The ratio of the intensity of the D band (I_d) to the intensity of the G

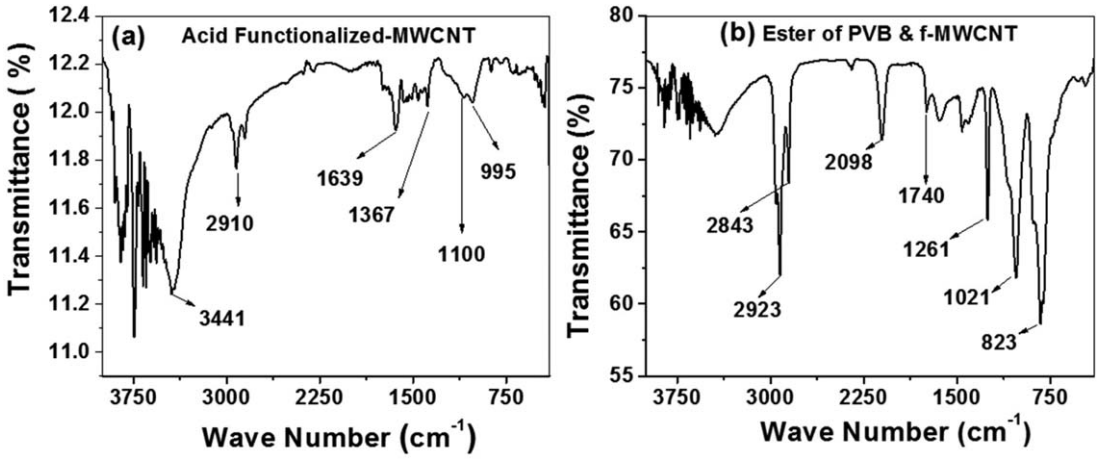

Figure 6. FTIR spectra of the (a) f-MWCNTs and (b) ester of PVB and f-MWCNT.

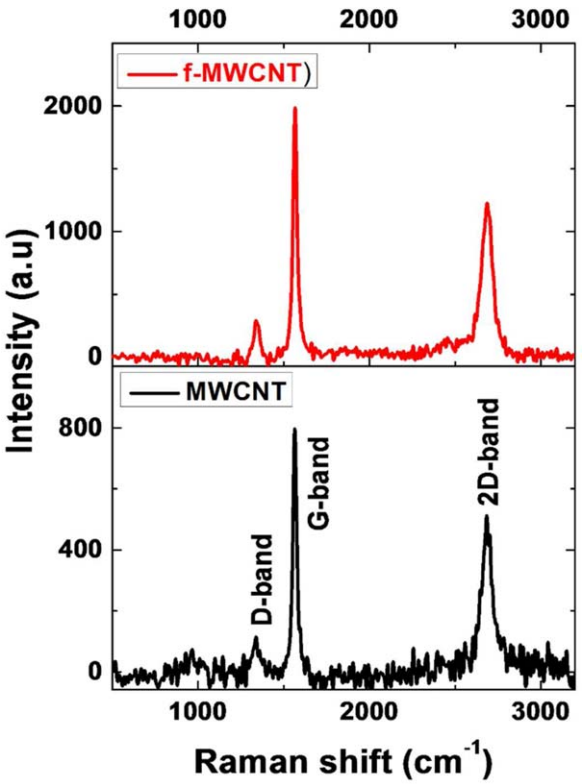

Figure 7. Raman spectra of the neat MWCNTs and f-MWCNTs. [Color figure can be viewed in the online issue, which is available at wileyonlinelibrary.com.]

band (I_g) gave us an idea about the defects present within the nanotubes. The calculated value of I_d/I_g for the neat MWCNTs and f-MWCNTs came out to be 0.143 and 0.147, respectively. When the I_d/I_g ratio was lower, there were fewer defects in the nanotubes. Hence, acid functionalization introduced defects in the nanotubes because of the incorporation of —COOH groups on the walls of nanotubes. Moreover, intensity of the Raman peaks increased in the f-MWCNTs compared to the MWCNTs; this indicated a higher purity of f-MWCNTs, as amorphous carbons were removed during the process of acid treatment.

Hydroxyl and Epoxy Group Equivalents

The hydroxyl and epoxy group equivalents of synthesized novolac and novolac epoxy resin were found to be 480 and 256.4 g/equivalent, respectively. The higher epoxy equivalent weight of synthesized novolac epoxy resin compared to the simple diglycidyl ether of bisphenol A (epoxy equivalent weight ≈ 180 g/equivalent) was attributed to the contribution of novolac resin to the molecular weight of the novolac epoxy resin. The further higher epoxy equivalent weight confirmed the reaction between epichlorohydrin and the novolac resin to form the novolac epoxy resin.

Thermal Analysis

TGA and derivative thermogravimetry (DTG) curves of the nanocomposites filled with f-MWCNTs and PVB are compared in Figure 8(i,iii). Figure 8(ii) demonstrates the TGA and DTG curves of the neat novolac epoxy and PVB. We observed from the DTG curves that the novolac epoxy resin and all of the nanocomposites showed two-step degradation processes, whereas for neat PVB, degradation occurs in only one step. The neat novolac epoxy resin showed its first peak degradation temperature (T_d^1) and second peak degradation temperature (T_d^2) at 380 and 405°C, respectively; these were associated with a 3.2 wt % residual yield at 900°C. This good thermal stability of the novolac epoxy resin was attributed to the high crosslinking density of the cured resin.[29] Neat PVB showed a degradation peak at 436°C with a residual yield of 2.1% at 600°C. The decomposition between 200 and 300°C was due to the decomposition of the hydroxyl group of PVB. The additional weight loss above 300°C was attributed to the decomposition of the butyral ring. The main decomposition in PVB was due to the removal of the butyral group.[30] We observed that all of the nanocomposites showed increasingly higher peak degradation temperatures compared to the neat novolac epoxy resin. This may have been because of the formation of chemical linkages between the —OH group of PVB and the —COOH group of f-MWCNTs. Moreover, acid functionalization also helped the MWCNTs to form chemical linkages with novolac epoxy resin; this also contributed to increments in the thermal stability. The initial small weight loss of the PVB-modified nanocomposites in the range 30–100°C was due to the removal of the solvents used to dissolve and disperse the PVB and f-MWCNTs within the novolac epoxy resin. Similar to the neat novolac epoxy resin, the decomposition of the nanocomposites containing f-MWCNTs and PVB occurred in two steps. The first weight loss took place in the range 330–400°C, whereas the second occurred between 400 and 475°C. From the TGA thermogram, it was clear that the residual yield increased from the neat novolac epoxy resin to the nanocomposites. However, the residual yield decreased with increasing PVB content. Among the nanocomposites, composite b showed the highest thermal stability and residue content (15.4%). For this composite, T_d^2 increased by 15°C compared to that of the neat novolac epoxy resin. This was attributed to the homogeneous dispersion of MWCNTs within the polymer matrix, as observed in its FESEM images. The TGA data of the neat novolac epoxy resin and its composites are presented in Table II.

Figure 9(i,ii) shows the MDSC of the nanocomposites, neat PVB, and novolac epoxy resin. The results of the analysis are shown in Table III. The neat novolac epoxy resin showed a glass-transition temperature (T_g) at 130.8°C; this conformed well with the reported value in the literature.[31] Neat PVB is a semicrystalline polymer. It showed a T_g, crystallization temperature, and melting point of 43, 56.7, and 65.3°C, respectively. We observed that at a low f-MWCNT loadings (viz., 0.1–0.25 wt %), the incorporation of PVB in the epoxy matrix shifted the T_g of the novolac epoxy towards lower temperatures because of the improvement in the segmental mobility of the epoxy matrix in the presence of PVB resin. Moreover, PVB resin decreased the crosslinking density of the novolac epoxy resin; this also contributed to the decrease in T_g.[31,32] At a 0.5 wt % f-MWCNT content, the decrease in T_g by the PVB was compensated by the improvement because of the presence of f-MWCNTs. Hence, the T_g value remained almost unchanged, as observed in the case of composite d. The improvement in the T_g of composite e could not be clearly understood and may have been due to the agglomeration of f-MWCNTs in the PVB phase by the preferential chemical reaction between the —COOH groups of the f-MWCNTs and the —OH groups of PVB

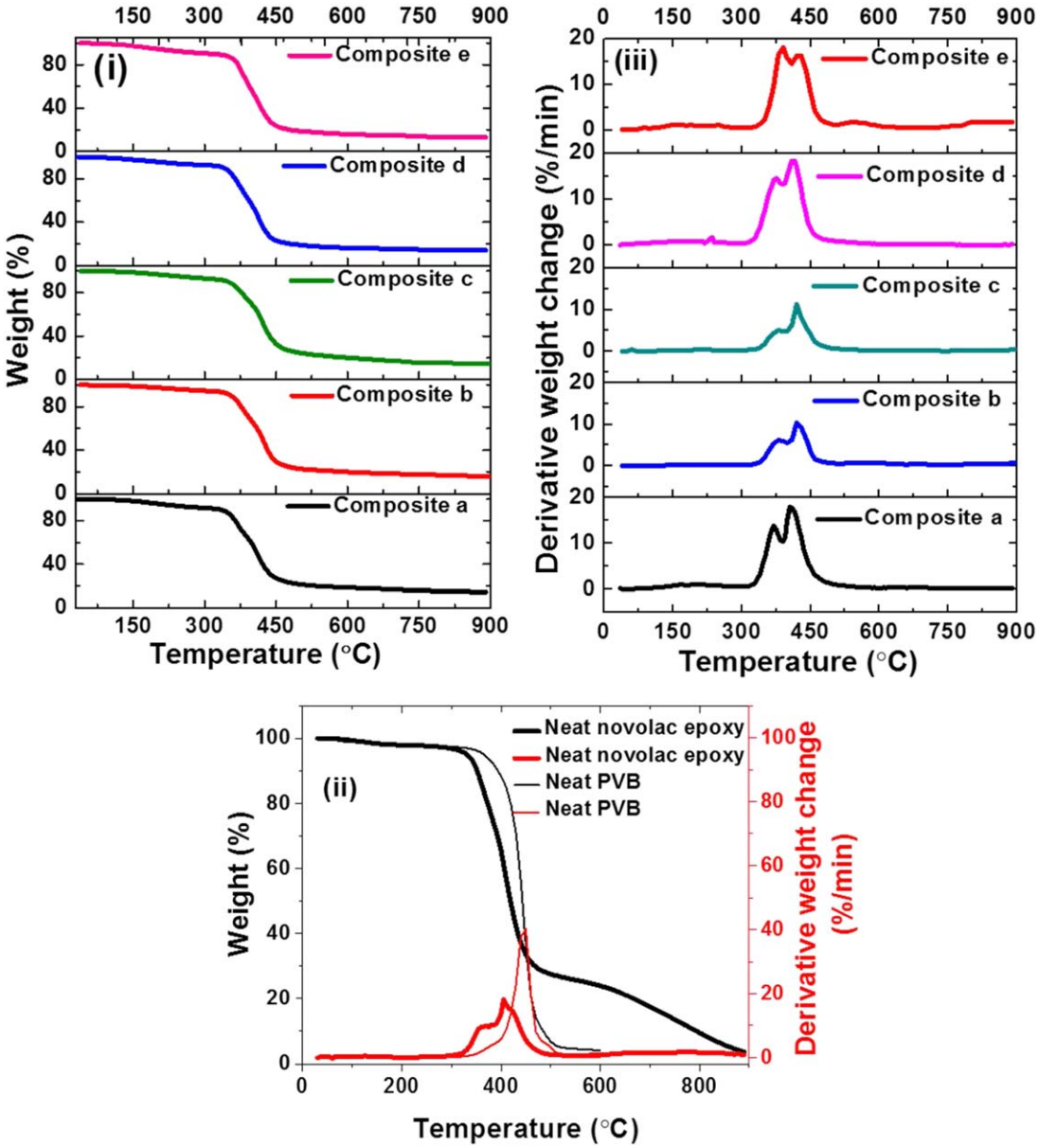

Figure 8. (i) TGA of the nanocomposites, (ii) TGA and DTG of the neat PVB and novolac epoxy, and (iii) DTG of nanocomposites. [Color figure can be viewed in the online issue, which is available at wileyonlinelibrary.com.]

Table II. Thermal Properties of the Neat Novolac Epoxy and Its Nanocomposites

Sample designation	T_d^1 (°C)	T_d^2 (°C)	Residual yield at 900°C (%)
Neat novolac epoxy	380	405	3.2
Neat PVB	436	—	2.1[a]
Composite a	370	405	14.5
Composite b	380	420	15.4
Composite c	380	420	14.2
Composite d	375	415	14.3
Composite e	380	420	12.9

[a] The residual yield for the neat PVB was reported at 600°C.

to form ester linkages. This was further supported by the FTIR analysis and the increase in T_g of the PVB phase, as shown in Table III. The crystallization temperature of the PVB phase in the nanocomposites increased gradually with increasing f-MWCNT content. This was attributed to the restriction imparted by the f-MWCNTs in the crystallization of the PVB molecular chain. A weak exothermic peak of the nanocomposites in the temperature range of about 232 to about 246°C accounted for the curing of traces of uncured novolac epoxy entrapped within the PVB polymer matrix.

Tensile Properties

The stress–strain characteristics of two representative specimens (having maximum and minimum elongations at break) of the neat novolac epoxy and nanocomposites are shown in Figure

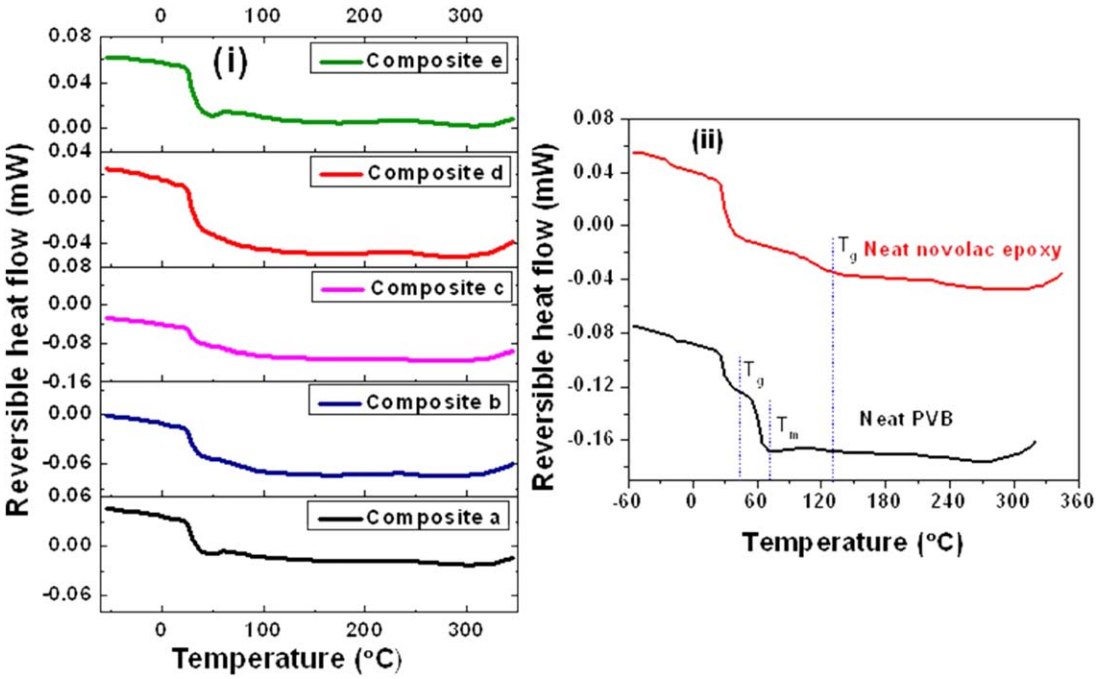

Figure 9. MDSC curves for the (i) nanocomposites and (ii) neat PVB and neat novolac epoxy. [Color figure can be viewed in the online issue, which is available at wileyonlinelibrary.com.]

10(a–f). Other specimens exhibited elongations at break between these two extreme values. We observed that in the case of the neat novolac epoxy, the slopes of the stress–strain curves were greater compared to that of the PVB-modified nanocomposites. Hence, the neat novolac epoxy showed highest tensile strength among all of the samples. However, it had the lowest elongation at break; this indicated its brittle characteristics. The effect of the PVB content on the tensile properties of the novolac epoxy nanocomposites is shown in Table IV. We observed that the elongation at break, tensile strength, and tensile modulus of the nanocomposites increased with increasing f-MWCNT loading up to 0.25 wt %. Composite b showed the highest tensile strength and modulus among the nanocomposites, whereas composite c exhibited the second highest tensile strength and modulus and best elongation at break among all of the nanocomposites. This was attributed to the homogeneous distribution of f-MWCNTs inside the polymer matrix, as observed in the FESEM images of both [see Figure 11(v,vi)]. At a 0.5 wt % f-MWCNT loading, the tensile strength and Young's modulus of the modified novolac epoxy nanocomposites decreased significantly compared to the neat novolac epoxy. This was attributed to the agglomeration of f-MWCNTs within the polymer matrix; this adversely affected the tensile properties of the nanocomposites. Moreover, the presence of thermoplastic PVB resin in the novolac epoxy matrix also contributed to such a reduction in the Young's modulus and strength of the nanocomposites because of their relatively low modulus and strength. Similar observations were also reported by Saleh *et al.*[33] for epoxy resin modified with the CTBN copolymer liquid rubber. PVB as the thermoplastic resin was not compatible with novolac epoxy resin, and hence, its presence led to heterogeneous dispersion at this small concentration, as evidenced from the FESEM images. The f-MWCNTs formed ester linkages with PVB, and were preferentially present in the PVB matrix at higher f-MWCNTs loadings (>0.25 wt %). Hence, the absence of a proper interface between the novolac epoxy matrix and PVB caused most of the nanocomposites to show inferior mechanical properties compared to that of the neat novolac epoxy. In addition, a small concentration of PVB acted as a defect and formed discrete patches within the

Table III. MDSC Results of the Neat Novolac Epoxy, Neat PVB, and Nanocomposites

Sample designation	T_g of PVB phase (°C)	T_g of novolac epoxy phase (°C)	Crystallization temperature of PVB (°C)	Melting temperature of PVB (°C)	Exothermic peak (°C)
Neat novolac epoxy	—	130.8	—	—	—
Neat PVB	43	—	56.7	65.3	
Composite a	45	129	58.6	—	245.7
Composite b	43	123	57.9	—	233
Composite c	43	127	58.9	—	243.6
Composite d	45	130	56.5	—	233.2
Composite e	44	137	59.5	—	232.6

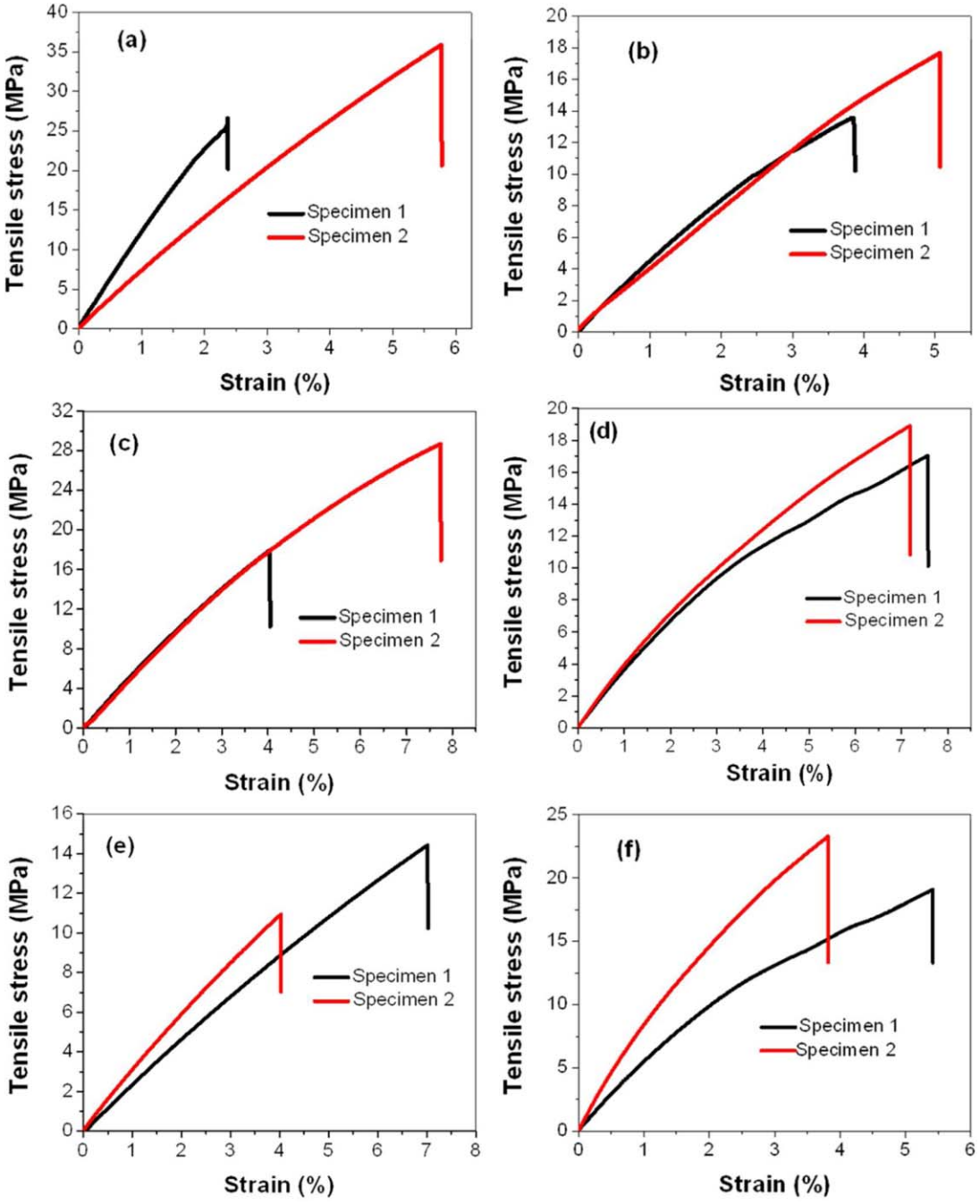

Figure 10. Stress–strain characteristics of the (a) neat novolac epoxy, (b) composite a, (c) composite b, (d) composite c, (e) composite d, and (f) composite e. [Color figure can be viewed in the online issue, which is available at wileyonlinelibrary.com.]

novolac epoxy matrix. This was observed in the FESEM images of the fractured surfaces of the Izod test specimens, as shown in Figure 11(iv,vii,viii). MWCNT-based epoxy nanocomposites have been studied by several researchers.[34,35] They observed that the mechanical properties of f-MWCNT-reinforced epoxy nanocomposites depended on the interfacial interaction and dispersion of the nanotubes within the epoxy matrix. The mechanical properties of the composites increased up to certain percentages (0.1–0.2%) of f-MWCNT loadings and decreased thereafter because of agglomeration. The elongation of the epoxy nanocomposites was reduced compared to that of the pure epoxy because of the restriction imparted by the nanofiller to the molecular chain stretching as the interfacial bonding strength (between the epoxy and nanofiller) increased significantly upon functionalization of the MWCNTs.

Flexural Properties

The experimental results of the flexural properties are shown in Table V. Similar to the tensile properties, the flexural strength and flexural modulus of the modified novolac epoxy

Table IV. Tensile Properties of the Neat Novolac Epoxy and Nanocomposites

Sample designation	Tensile strength at maximum load (MPa)	Tensile strength at break (MPa)	Elongation at break (%)	Modulus (MPa)
Neat novolac epoxy	31.3 ± 3.0	31.3 ± 3.0	4.1 ± 1.0	743.1 ± 7.2
Composite a	15.9 ± 1.6	15.6 ± 1.5	4.6 ± 0.4	417.9 ± 5.4
Composite b	23.3 ± 2.2	23.3 ± 2.2	5.9 ± 0.5	1776 ± 10
Composite c	20.3 ± 2.0	20.3 ± 2.0	7.4 ± 0.7	1158.4 ± 8.8
Composite d	12.3 ± 1.5	11.9 ± 1.4	5.3 ± 0.6	302 ± 4.2
Composite e	21.8 ± 1.8	20.2 ± 1.7	4.4 ± 0.7	582.8 ± 6

nanocomposites were reduced compared to that of the neat novolac epoxy, except for composite b, which showed a greater flexural strength than the neat novolac epoxy. This was due to the heterogeneous distribution of PVB resin in the continuous novolac epoxy matrix and the agglomeration of f-MWCNTs at higher filler loadings. Composite b exhibited the highest flexural strength among all of the nanocomposites. This result conformed well to the tensile properties of the nanocomposites.

Impact Properties

The impact properties of the nanocomposites are presented in Table VI. Furthermore, experimental observations of the impact properties of the neat novolac epoxy resin and its nanocomposites could be explained on the basis of the FESEM images of the fractured surfaces of the Izod test samples, as shown in Figure 11 (see Morphology of the Nanocomposites section). In general, the Izod impact strengths of the PVB-modified nanocomposites, except for that of composite c, were smaller than that of neat novolac epoxy resin. This was due to the lower concentration of PVB, which formed discrete patches in the novolac epoxy matrix, and therefore, the domain size of PVB became larger than the required domain size for better impact properties. We know from the literature that for better impact properties, the size of the dispersed phase should be between 250 and 370 nm.[36] Hence, the larger size of the dispersed PVB phase inside the novolac epoxy matrix could have been the possible reason for such a decrement, as this acted as the stress concentration point during the impact analysis. It was also clear from the FESEM images of the nanocomposites that because of the greater compatibility of the f-MWCNTs with PVB compared

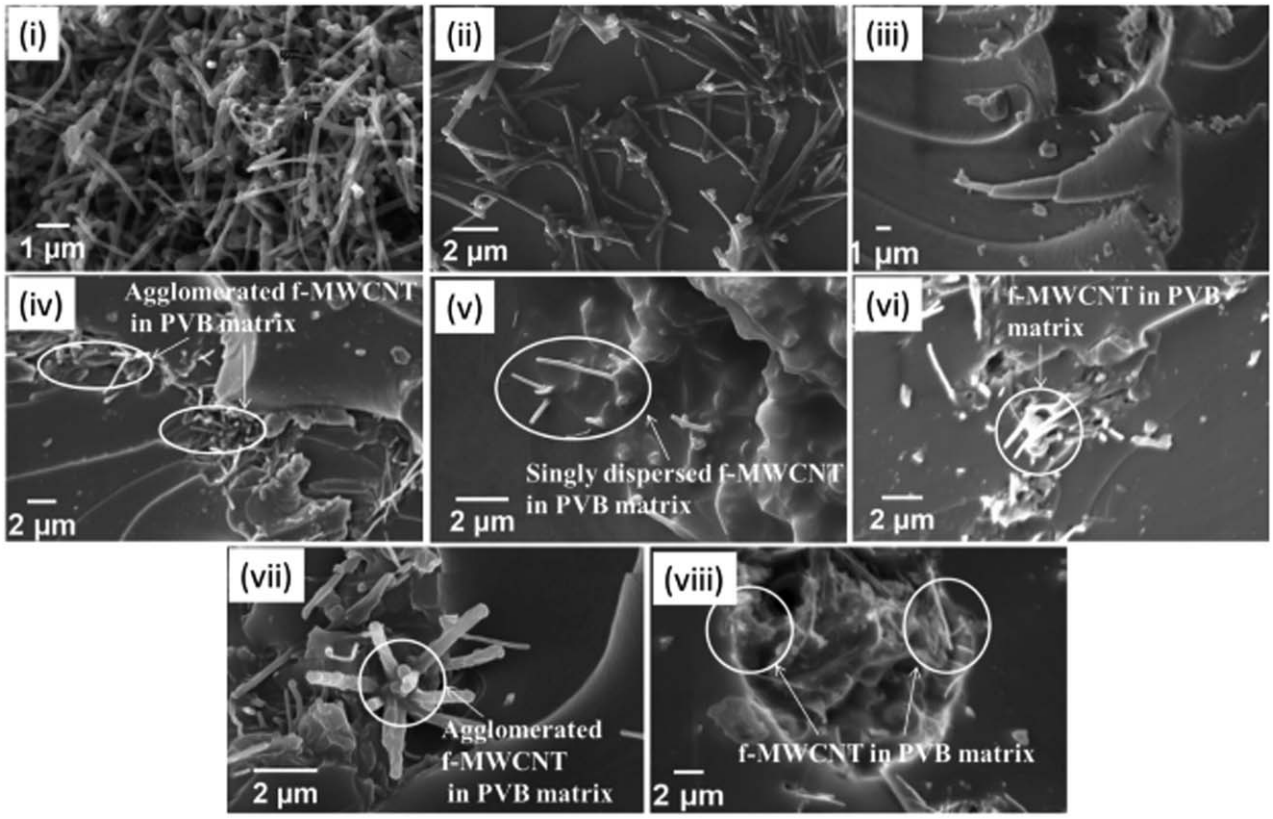

Figure 11. FESEM images of the (i) crude MWCNTs, (ii) f-MWCNTs, and fractured impact specimen surfaces of the (iii) neat novolac epoxy, (iv) composite a, (v) composite b, (vi) composite c, (vii) composite d, and (viii) composite e.

Table V. Flexural Properties of the Neat Novolac Epoxy and Nanocomposites

Sample designation	Flexural strength at maximum load (MPa)	Flexural modulus (GPa)
Neat novolac epoxy	70.3 ± 5.5	3.5 ± 0.06
Composite a	31.1 ± 4.5	1.2 ± 0.1
Composite b	71.1 ± 3	2.4 ± 0.08
Composite c	55.5 ± 0.5	1.9 ± 0.1
Composite d	68.5 ± 5.0	2.8 ± 0.12
Composite e	21.0 ± 2.5	1.2 ± 0.1

to the novolac epoxy resin, the f-MWCNTs concentrated in the PVB phase, and this led to their agglomeration as the PVB concentration was increased. Further, this may have been because of the chemical reaction of the f-MWCNTs with the —OH group of the PVB to form esters of MWCNTs, as discussed in the FTIR Spectroscopy section. The formation of esters rendered the PVB insoluble in epoxy, and a phase-separated morphology was generated. Therefore, the incorporation of PVB and f-MWCNTs negatively affected the impact properties of the nanocomposites at higher concentrations. The highest impact properties of composite c may have originated from the better dispersion and homogeneity of the f-MWCNTs within the novolac epoxy matrix, as shown in its FESEM images [see Figure 11(vi)]. The highest impact strength in composite c was further supported by its highest elongation at break and toughness, as discussed in the Tensile Properties section.

Morphology of the Nanocomposites

FESEM images of the neat MWCNTs and f-MWCNTs are shown in Figure 11(i,ii). The neat MWCNTs existed as entangled clusters of nanotubes, whereas these clusters are dispersed in the f-MWCNTs as a result of acid treatment. After acid treatment, the smooth surfaces of the MWCNTs turned out to be rough because of the introduction of defects on the side wall, and their length was reduced compared to that of the neat MWCNTs.[37,38] Figure 11(iii) shows the FESEM image of the Izod impact test sample fracture surface for the neat novolac epoxy resin, and Figure 11(iv–viii) shows those of composites a–e, respectively.

We observed that the fracture mechanism for the neat novolac epoxy resin was governed by the brittle failure. For nanocomposites, the failure pattern gradually changed from brittle failure to ductile failure. However, because of the noncompatibility of the epoxy and PVB matrix, the formation of the interface was not observed. This is why most of the nanocomposites showed inferior mechanical properties (Izod impact strength and tensile and flexural properties) compared to that of the neat novolac epoxy. In the case of composite b, the f-MWCNTs were dispersed homogeneously throughout the polymer matrix and were pulled out from the matrix during the mechanical testing; this indicated better interfacial bonding between them. This phenomenon was further supported by its superior mechanical properties. At higher f-MWCNT loadings (i.e., 0.5 wt %), the aggregation of the nanotubes took place, and this led to the heterogeneous dispersion of nanotubes, as shown in Figure 11(iv,vii,viii). Hence, the nanocomposites were characterized by the localized presence of PVB as the discrete phase inside the novolac epoxy resin. Moreover, the presence of f-MWCNTs was observed to be greater in the PVB phase compared to the novolac epoxy resin phase. This led to the heterogeneous dispersion of PVB and f-MWCNTs inside the novolac epoxy resin and rendered the generation of weak interfaces and led to inferior mechanical properties at higher f-MWCNT loadings.

Table VI. Impact Properties of the Neat Novolac Epoxy and Its Nanocomposites

Sample designation	Impact strength (kJ/m^2)
Neat novolac epoxy	13.5 ± 1.8
Composite a	6.2 ± 0.6
Composite b	11.1 ± 1.4
Composite c	17.0 ± 0.8
Composite d	12.7 ± 1.6
Composite e	8.7 ± 0.7

CONCLUSIONS

In this article, we have reported the effects of PVB modification on the thermal and mechanical characteristics of novolac epoxy and functionalized-CNT-based nanocomposites. The blending of a small amount of PVB with a thermosetting novolac epoxy resin resulted in a loss of mechanical properties in the nanocomposites because of the low modulus and noncompatibility of the PVB resin with the host novolac epoxy resin. PVB formed a discrete localized phase inside the novolac epoxy resin; this acted as the stress concentration point and led to the easy failure of the nanocomposites during mechanical testing. The incorporation of the functionalized CNTs was observed to be successful in improving the thermal and mechanical properties at low concentrations (between 0.1 and 0.25 wt %). The nanocomposite containing 1.5 wt % PVB and 0.1 wt % CNTs showed the best tensile and flexural properties among the nanocomposites; however, the best elongation and impact properties were achieved in the nanocomposite containing 1.5 wt % PVB and 0.25 wt % functionalized CNTs. T_g of the novolac epoxy phase decreased with increasing PVB content but increased with increasing nanotube content. The peak degradation temperature increased by 15°C in the nanocomposite containing 1.5 wt % PVB and 0.1 wt % functionalized CNTs because of the homogeneous dispersion of nanotubes at low concentrations.

ACKNOWLEDGMENTS

The authors are obliged to the director of the Defence Material and Stores Research & Development Establishment (Kanpur, India) for providing the laboratory facilities for this research work. The authors also acknowledge the Central Institute of Plastics Engineering and Technology (Lucknow, India) and the Rubber & Adhesive Division of the Defence Material and Stores Research & Development Establishment for their support in mechanical characterization.

REFERENCES

1. Nair, C. P. *Prog. Polym. Sci.* **2004**, *43*, 401.
2. Das, G.; Karak, N. *Prog. Org. Coat.* **2010**, *69*, 495.
3. Sudhakara, P.; Kannan, P.; Obireddy, K.; Varadarajulu, A. *J. Mater. Sci.* **2011**, *46*, 2778.
4. Chonkaew, W.; Sombatsompop, N.; Brostow, W. *Eur. Polym. J.* **2013**, *43*, 1461.
5. Lu, S.; Ban, J.; Yu, C.; Deng, W. *Iran. Polym. J.* **2010**, *19*, 669.
6. Takahashi, Y. J. *J. Appl. Polym. Sci.* **1961**, *5*, 468.
7. Salimi, A.; Omidian, H.; Zohuriaan-Mehr, M. J. *J. Adhes. Sci. Technol.* **2003**, *17*, 1847.
8. Sulton, J. N.; Carry, F. J. *J. Polym. Eng. Sci.* **1973**, *23*, 29.
9. Yishi, S.; Shiqi, Z.; Xiuying, L.; Xiqun, W. *Chin. J. Polym. Sci.* **1987**, *3*, 229.
10. Bascom, W. D.; Cottington, R. L. *J. Sci. Adhes.* **1976**, *7*, 333.
11. Chonkaew, W.; Sombatsompop, N. *J. Appl. Polym. Sci.* **2012**, *125*, 361.
12. Mathew, V. S.; Jyotishkumar, P.; George, S. C.; Gopalakrishnan, P.; Delbreilh, L.; Saiter, J. M.; Saikia, P. J.; Thomas, S. *J. Appl. Polym. Sci.* **2012**, *125*, 804.
13. Jyotishkumar, P.; Pionteck, J.; Moldenaers, P.; Thomas, S. *J. Appl. Polym. Sci.* **2012**, *127*, 3093.
14. Thomas, R.; Boudenne, A.; Ibos, L.; Candau, Y.; Thomas, S. *J. Appl. Polym. Sci.* **2010**, *116*, 3232.
15. Jin, F.; Park, S. *Carbon Lett.* **2011**, *12*, 57.
16. Ramana, G.; Padya, B.; Kumar, R.; Prabhakar, K.; Jain, P. *Indian J. Eng. Mater. Sci.* **2010**, *17*, 331.
17. Hamdani, N.; Najim, T.; Khlaf, F. *J. Appl. Phys.* **2014**, *6*, 50.
18. Dehghan, M.; Al-Mahaidi, R.; Sbarski, I. *Int. J. Chem. Nucl. Mater. Metall. Eng.* **2014**, *8*, 119.
19. Sabarinathan, C.; Muthu, S.; Ali, M. N. *J. Appl. Sci. Res.* **2012**, *8*, 3253.
20. Mordina, B.; Tiwari, R. K.; Setua, D. K.; Sharma, A. *J. Phys. Chem. C* **2014**, *118*, 25684.
21. Mordina, B.; Tiwari, R. K.; Setua, D. K.; Sharma, A. *RSC Adv.* **2015**, *5*, 19091.
22. Khanam, A.; Mordina, B.; Tiwari, R. K. *J. Compos. Mater.* **2015**, *49*, 2497.
23. Mordina, B.; Tiwari, R. K. *J. Compos. Mater.* **2012**, *47*, 2835.
24. Kurahatti, R. V.; Suredranathan, A. O.; Kori, S. A.; Kumar, A. V. R.; Mordina, B.; Mallapur, D. G. *Tribology* **2011**, *5*, 49.
25. Saleh, A. B.; Mohd Ishak, Z. A.; Hashim, A. S.; Kamil, W. A. *J. Phys. Sci.* **2009**, *20*, 1.
26. Kumar, H.; Tripathi, S. K.; Mistry, S.; Bajpai, G. D. E *J. Chem.* **2009**, *6*, 1253.
27. Amiriana, M.; Chakolia, A. N.; Caia, W.; Suia, J. *Sci. Iran.* **2013**, *20*, 1023.
28. Lehman, J. H.; Terrones, M.; Mansfield, E.; Hurst, K. E.; Meunier, V. *Carbon* **2011**, *49*, 2581.
29. Liu, Y.; Du, Z.; Zhang, C.; Li, C. *J. Appl. Polym. Sci.* **2007**, *103*, 2041.
30. Zanjanijiam, A. R.; Hajian, M.; Koohmareh, G. A. *J. Appl. Polym. Sci.* **2014**, *131*, 1.
31. Vijayan, P. P.; Pionteck, J.; Huczko, A.; Puglia, D.; Kenny, J. M.; Thomas, S. *Compos. Sci. Technol.* **2014**, *102*, 65.
32. Zhang, Xi.; Yan, X.; Guo, J.; Liu, Z.; Jiang, D.; He, Q.; Wei, H.; Gu, H.; Colorado, H. A.; Zhang, X.; Wei, S.; Guo, Z. *J. Mater. Chem. C* **2015**, *3*, 162.
33. Ben Saleh, A. B.; Mohd Ishak, Z. A.; Hashim, A. S.; Kamil, W. A. *J. Phys. Sci.* **2009**, *20*, 1.
34. Salam, M. B. A.; Hosur, M. V.; Zainuddin, S.; Jeelani, S. *Open J. Compos. Mater.* **2013**, *3*, 1.
35. Al-Hamdani, N. A.; Najim, T. S.; Khlaf, F. A. *IOSR J. Appl. Phys.* **2014**, *6*, 50.
36. Borggreve, R. M.; Gaymans, R. *J. Polymer* **1989**, *30*, 63.
37. Khani, H.; Moradi, O. *J. Nanostruct. Chem.* **2013**, *3*, 1.
38. Pisal, S. H.; Harale, N. S.; Bhat, T. S.; Deshmukh, H. P.; Patil, P. S. *J. Appl. Chem.* **2014**, *7*, 49.